Journal of Solid Mechanics Vol. 7, No. 3 (2015) pp. 239-254

Axial and Transverse Vibration of SWBNNT System Coupled Pasternak Foundation Under a Moving Nanoparticle Using Timoshenko Beam Theory

A. Ghorbanpour Arani [1, 2, *], A. Karamali Ravandi [1], M.A. Roudbari [1], M.B. Azizkhani [1], A. Hafizi Bidgoli [1]

[1] *Faculty of Mechanical Engineering, University of Kashan, Kashan , Islamic Republic of Iran*
[2] *Institute of Nanoscience & Nanotechnology, University of Kashan, Kashan, Islamic Republic of Iran*

Received 23 March 2015; accepted 22 May 2015

ABSTRACT

In this study, a semi analytical method for transverse and axial vibration of single-walled boron nitride nanotube (SWBNNT) under moving a nanoparticle is presented. The surrounding elastic medium as Pasternak foundation and surface stress effect are included in the formulations of the proposed model. Using Timoshenko beam theory (TBT), Hamilton's principle and nonlocal piezoelasticity theory, the higher order governing equation is derived. The influences of surface stress effects, spring and shear parameters of Pasternak foundation and aspect ratio are also investigated on the free and forced vibration behavior of SWBNNT under moving a nanoparticle. Through an inclusive parametric study, the importance of using surrounding elastic medium in decrease of normalized dynamic deflection is proposed. It is demonstrated that the values of shear modulus have significant role on the vibration behavior of SWBNNT. The influences of surface stresses on the amplitude of normalized dynamic deflection are also discussed. The output result's of this study has significant influences in design and production of micro electro mechanical system (MEMS) and nano electro mechanical system (NEMS) for advanced applications.

Keywords : Axial and transverse vibration; SWBNNT; Nanoparticle; Piezoelastic theory; Pasternak foundation; Surface stress effect.

1 INTRODUCTION

IN recent years, two great groups of nanotubes have been introduced by researchers such as carbon nanotubes (CNTs) and boron nitride nanotubes (BNNTs). The structure of CNTs and BNNTs are same in which carbon atoms are substituted by alternating boron (B) and nitrogen (N) atoms. They are different as far as higher temperature resistance to oxidation more than $900^{\circ}C$ and possessing strong piezoelectric characteristics are concerned. The electrical properties of the CNTs are strongly affected by the rolling angle of the nanotube lattice molecular structure known as chirality which has limited the applications of CNTs in electrical components, especially in nanoelectrical devices. But, because of the large band gaps regardless of chirality and diameter BNNTs are semiconductors. So they play a dominant role as a significant material to be used for nano sensors and actuators,

* Corresponding author. Tel.: +98 31 55912450; Fax: +98 31 55912424.
E-mail address: aghorban@kashanu.ac.ir (A. Ghorbanpour Arani).

due to their unique structural properties. BN structures are useful in design and manufacturing of nano devices such as MEMS and NEMS. The mechanical, thermal, physical and chemical properties of piezoelectric materials such as high elastic modulus, low density, high thermal conductivity, constant wide band gap, superb structural stability and chemical inertness has made intense enthusiasm for researchers to investigate all aspects of such structures built up by BN. In recent years, so many papers have been carried out on the buckling, instability, vibration and wave propagation of nanotubes/microtubes in the literature. Khoddami Maraghi et al. [1] reported nonlocal vibration and instability of embedded DWBNNT conveying viscose fluid. Simsek [2- 3] studied forced vibration of an embedded single-walled carbon nanotube traversed by a moving load using nonlocal elasticity theory for both Euler-Bernoulli and Timoshenko beam theories. He showed that the nonlocal parameter and shear deformation have greatly affects on the dynamic behavior of the nanotube with lower aspect ratios and cannot be neglected in the analysis of short nanotubes. Ghorbanpour Arani et al. [4] investigated nonlocal vibration of SWBNNT embedded in bundle of CNTs under a moving nanoparticle. Recently, surface stress effect has been considered in some research works. Bending behavior and buckling of nanobeams including surface stress effects corresponding to different beam theories has been proposed by Ansari et al. [5]. Also, in another paper, he investigated the surface stress effects on the free vibration behavior of nanoplates [6]. Lei et al. [7] studied surface effects on the vibrational frequency of DWCNTs using the nonlocal Timoshenko beam model. They found that in short DWCNTs, the influence of surface stress on the vibration behavior is pronounced. Study of nonlocal wave properties of nanotubes with surface effects was presented by Narendar et al. [8].

Most of the recent research is limited to CNTs, but few studies dealing with BNNTs as smart nanotube in the published literature.Electro-thermo-nonlocal transverse vibration behavior of DWBNNTs embedded in an elastic medium using nonlocal piezoelasticity theory was studied by Ghorbanpour Arani et al. [9] who showed the effects of electric field and temperature change on the frequency. Also, Ghorbanpour Arani et al. [10] presented the buckling of embedded DWBNNTs under combined electro-thermo-mechanical loadings. They concluded that the electricfield and its direction have been affected by the magnitude of the critical buckling load.

Based on the author's knowledge, there is no detailed investigation on the dynamic effects of the moving nanoparticles in the BNNT structures using TBT in the literature. Motivated by these considerations and the importance of using BNNTs instead of CNTs, this study aims to propose the evaluation of a SWBNNT surrounded by Pasternak foundation using nonlocal piezoelasticity for TBT theory under a moving nanoparticle. Using Hamilton's principle, the governing equations are derived. The effects of velocity parameter of nanoparticle, elastic and shear modulus and surface stress on the vibration of the SWBNNTs are discussed in details.

2 MODELING OF SWBNNT VIA NONLOCAL TBT

2.1 Basic formulation

Consider a SWBNNT including a moving nanoparticle surrounded by Pasternak foundation as illustrated in Fig. 1. The inner and outer radius, the length and the thickness of nanotube are R_{in}, R_{out}, L and t_n, respectively.

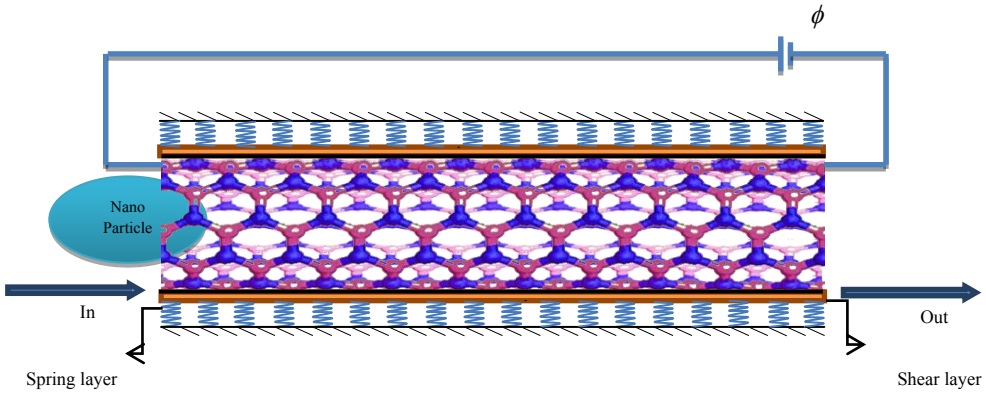

Fig.1
Configuration of a SWBNNT under moving a nanoparticle surrounded by Pasternak foundation and with applied electric field.

2.2 A review on piezoelasticity theory

Since BNNTs are piezoelectric materials, the constitutive equation of piezoelasticity theory must be used as follows [11]:

$$\{\sigma\} = [C]\{\varepsilon\} - [h]^T \{E\} \qquad \{D\} = [h]^T \{\varepsilon\} + [\in]\{E\} \tag{1}$$

where $\{\sigma\},\{\varepsilon\},\{E\}$ and $\{D\}$ are classical stress, strain, electric field and displacement fields, respectively. Likewise $[C],[h]^T$ and $[\in]$ denote elastic stiffness, piezoelectric and dielectric parameters, respectively. $[C]$ for an orthotropic material needs 9 independent matrix entries and can be expanded as [1]:

$$[C] = \begin{bmatrix} c_{11} & c_{12} & c_{13} & 0 & 0 & 0 \\ c_{21} & c_{22} & c_{23} & 0 & 0 & 0 \\ c_{31} & c_{32} & c_{33} & 0 & 0 & 0 \\ 0 & 0 & 0 & c_{44} & 0 & 0 \\ 0 & 0 & 0 & 0 & c_{55} & 0 \\ 0 & 0 & 0 & 0 & 0 & c_{66} \end{bmatrix} \tag{1a}$$

$$\begin{aligned} C_{11} &= C_{22} = C_{33} = \frac{E}{1-\nu^2} \\ C_{12} &= C_{13} = C_{23} = \frac{\nu E}{1-\nu^2} \\ C_{44} &= C_{55} = C_{66} = G \end{aligned} \tag{1b}$$

where E ,G and υ are Young's modulus, shear modulus and Poisson ratio, respectively. We use zigzag structure of BNNTs because of their favorable response to tension and compression loadings. $[h]^T$ and $[\in]$ may be written as [1]:

$$[h]^T = \begin{bmatrix} h_{11} & 0 & 0 \\ 0 & 0 & 0 \\ 0 & 0 & 0 \\ 0 & 0 & 0 \\ 0 & 0 & 0 \\ 0 & 0 & 0 \end{bmatrix} \quad , \quad [\in] = \begin{bmatrix} \in_{11} & 0 & 0 \\ 0 & 0 & 0 \\ 0 & 0 & 0 \end{bmatrix} \tag{1c}$$

Electric field is being expanded as:

$$\{E\} = \begin{Bmatrix} E_x \\ E_\Theta \\ E_z \end{Bmatrix} \tag{2}$$

According to TBT, displacement field can be considered as:

$$\tilde{u}(x,z,t) = u(x,t) + z\psi(x,t) \quad , \tilde{v}(x,z,t) = 0 \quad , \tilde{w}(x,z,t) = w(x,t) \tag{3}$$

where $u(x,t)$, $w(x,t)$ and $\psi(x,t)$ are axial, transverse displacement and rotational angle of neutral axis, respectively.

Linear kinematic relation in this model may be written as:

$$\varepsilon_{xx} = \frac{\partial}{\partial x} u(x,t) + z \frac{\partial}{\partial x} \psi(x,t) \qquad \gamma_{xz} = \frac{\partial w(x,t)}{\partial x} + \psi(x,t) \tag{4}$$

On the other hand, for this particular problem, constitutive equations introduced in Eq. (1) can be rewritten as follows:

$$\sigma_{xx} = c_{11}\varepsilon_{xx} - h_{11}E_x \qquad \sigma_{xz} = c_{55}\left(\frac{\partial w}{\partial x} + \psi\right) \qquad D_{xx} = h_{11}\varepsilon_{xx} + \in_{11} E_x \tag{5}$$

and E_x is given as follows [12]:

$$E_x = -\frac{\partial}{\partial x}\phi(x,t) \tag{6}$$

where ϕ denotes electrical potential.

2.3 Equations of motion derivation procedure

In this work, in order to obtain the equations of motion, Hamilton principle is used. Before applying this method, the following preliminary functions should be calculated:

a) Potential strain energy:

$$U_s = \frac{1}{2}\int_0^L \iint_A \left(\sigma_{xx}\varepsilon_{xx} + 2\sigma_{xz}\varepsilon_{xz} - D_x E_x\right) dA dx \tag{7}$$

b) Kinematic energy function:

$$K_{tube} = \frac{1}{2}\int_0^L \iint_A \rho\left[\left(\frac{\partial \tilde{u}}{\partial t}\right)^2 + \left(\frac{\partial \tilde{w}}{\partial t}\right)^2\right] dA dx \tag{8}$$

where A and ρ denotes section area and mass density of nanotube, respectively. The components of integral arguments introduced in Eqs. (7) and (8) must be replaced by their equivalents defined in Eqs. (4), (5) and (6).

c) Work of external forces:

The external forces applied to system are due to Pasternak foundation and nanoparticle movement and can be written as [4]:

$$F_{elastic} = k_w w - G_p \nabla^2 w - P \tag{9}$$

where k_w and G_p are spring and shear modulus of Pasternak foundation, respectively. The force P is considered mainly as an impulse function by papers published in the literature [13]:

$$P = P_0 \delta(x - x_{np}) \tag{10}$$

In this simulation, p_0 is the magnitude of the force induced by moving load, δ indicates Dirac-delta function and x_{np} represents the position of nanoparticle in the BNNT. Thus, the work done by external forces can be expressed as:

$$\Omega = \frac{1}{2}\int_0^L \left(-k_w w + G_p \nabla^2 w + P\right) w dx \tag{11}$$

Minimum potential energy principle, known as Hamilton principle in dynamic systems and structures are given by:

$$\delta\Pi = 0 \tag{12}$$

where potential energy, Π, is defined as:

$$\Pi = U - K - \Omega \tag{13}$$

Substituting Eqs. (7), (8) and (11) into (13) and then into (12), the final local form of motion equations are obtained as follows:

$$\begin{aligned}
&\delta u : \frac{\partial N_x}{\partial x} + h_{11} A \frac{\partial^2 \varphi}{\partial x^2} - 2 m_t \frac{\partial^2 u}{\partial t^2} = 0 \\
&\delta w : -\frac{\partial Q_x}{\partial x} + m_t \frac{\partial^2 w}{\partial t^2} + k_w w - G_p \nabla^2 w - \frac{1}{2} p = 0 \\
&\delta\psi : -\frac{1}{2}\frac{\partial M_x}{\partial x} + Q_x + \rho I \frac{\partial^2 \psi}{\partial t^2} = 0 \\
&\delta\phi : h_{11} A \frac{\partial^2 u}{\partial x^2} - 2A \in_{11} \frac{\partial^2 \varphi}{\partial x^2} = 0
\end{aligned} \tag{14}$$

where $m_t = \rho A$ is the BNNT mass per length of nanotube and stress resultants are defined as:

$$N_x = \int_A \sigma_{xx} dA \,,\; M_x = \int_A z\sigma_{xx} dA \,,\; Q_x = \int_A \sigma_{xz} dA \tag{15}$$

3 NONLOCAL PEIZOELACTICITY THEORY

According to the nonlocal elasticity theory [14], the stress field at a point *x* in an elastic continuum not only depends on the strain field at the same point but also on strain at all other points of the body. The constitutive equation of the nonlocal elasticity then becomes:

$$\left(1 - \left(e_0 a\right)^2 \nabla^2\right) \sigma^{nl} = \sigma^{l} \tag{16}$$

where ∇^2 denotes Laplacian operator, σ^{nl} and σ^{l} are nonlocal and local stress fields, respectively. Eq. (14) has been widely used for the study of micro and nanostructure elements. Therefore, non-zero nonlocal stresses and flux density correspondence to nanotube structures are outlined as:[1, 4, 14]

$$\sigma_{xx}^{nl}-\left(e_0a\right)^2\sigma_{xx}^{nl}=c_{11}\varepsilon_{xx}-h_{11}E_x \qquad \sigma_{xz}^{nl}-\left(e_0a\right)^2\sigma_{xz}^{nl}=c_{55}\left(\frac{\partial w}{\partial x}+\psi\right)$$
$$D_{xx}^{nl}-\left(e_0a\right)^2 D_{xx}^{nl}=h_{11}\varepsilon_{xx}+\in_{11} E_x \tag{17}$$

Using Eqs. (14), (15) and (17) and doing some arithmetic operations, the final nonlocal forms of motion equations can be obtained as follows:

$$\begin{aligned}
&\delta u: -c_{11}A\frac{\partial^2 u}{\partial x^2}-h_{11}A\frac{\partial^2\varphi}{\partial x^2}+\mu h_{11}A\frac{\partial^4\varphi}{\partial x^4}+2m_t\frac{\partial^2 u}{\partial t^2}-2\mu m_t\frac{\partial^4 u}{\partial x^2\partial t^2}=0\\
&\delta w: \mu m_t\frac{\partial^4 w}{\partial x^2\partial t^2}-\mu\left(G_p\frac{\partial^4 w}{\partial x^4}+p''-k_w\frac{\partial^2 w}{\partial x^2}\right)+k_sGA\left(\frac{\partial^2 w}{\partial x^2}+\frac{\partial\psi}{\partial x}\right)-m_t\frac{\partial^2 w}{\partial t^2}-k_w w+G_p\frac{\partial^2 w}{\partial x^2}+p=0\\
&\delta\psi: k_sGA\left[\frac{\partial w}{\partial x}+\psi\right]-\rho I\mu\frac{\partial^2\psi}{\partial x^2\partial t^2}-\frac{1}{2}c_{11}I\frac{\partial^2\psi}{\partial x^2}+\rho I\frac{\partial^2\psi}{\partial t^2}=0\\
&\delta\phi: h_{11}A\frac{\partial^2 u}{\partial x^2}-\mu h_{11}A\frac{\partial^4 u}{\partial x^4}-2\in_{11}A\frac{\partial^2\varphi}{\partial x^2}+2\mu\in_{11}A\frac{\partial^4\varphi}{\partial x^4}=0
\end{aligned} \tag{18}$$

The coefficients of δw and $\delta\psi$ considering surface stress effect in final form can be rewritten as:

$$\begin{aligned}
&\delta w: \mu m_t\frac{\partial^4 w}{\partial x^2\partial t^2}-\mu\left(\left(G_p+H_i\right)\frac{\partial^4 w}{\partial x^4}+p''-k_w\frac{\partial^2 w}{\partial x^2}\right)+k_sGA\left(\frac{\partial^2 w}{\partial x^2}+\frac{\partial\psi}{\partial x}\right)\\
&-m_t\frac{\partial^2 w}{\partial t^2}-k_w w+\left(G_p+H_i\right)\frac{\partial^2 w}{\partial x^2}+p=0
\end{aligned} \tag{19}$$

$$\delta\psi: k_sGA\left[\frac{\partial w}{\partial x}+\psi\right]-\rho I\mu\frac{\partial^2\psi}{\partial x^2\partial t^2}-\frac{1}{2}\frac{\left(EI\right)_i^*}{1-\upsilon^2}\frac{\partial^2\psi}{\partial x^2}+\rho I\frac{\partial^2\psi}{\partial t^2}=0 \tag{20}$$

where $\left(EI\right)_i^*$ and H_i are defined as follows [7]:

Inner radius $\left(EI\right)_1^*=EI \qquad H_1=0$

Outer radius $\left(EI\right)_2^*=EI+\pi E^s R_{out}^3 \qquad H_2=4\tau R_{out}$

where E^s and τ are the surface elasticity modulus and the residual surface tension per length, respectively [7].In this paper, an analytical solution is developed to calculate natural frequency of transverse and axial vibrations, and a numerical solution, namely constant average acceleration method proposed by Newmark has been adopted to calculate dimensionless amplitude of vibration. Also, the following assumptions are supposed:

i. Boundary conditions in both sides of BNNT are simply supported.
ii. The velocity of nanoparticle is constant.
iii. The friction force between the outer surface of nanoparticle and inner surface of the BNNT is neglected.
iv. The inertial effect of the nanoparticle is negligible.
v. Initial displacement and velocity of BNNT are zero before arrival of nanoparticle.

4 ANALYTICAL SOLUTION

Analytical solution is developed due to investigation of free vibration analysis and also to find natural frequency ω. The total dynamic transverse and axial deflection in modal form can be written as:

$$W(x,t)=\sum_{m=1}^{\infty}\eta_m(x)f_m(t) \qquad , \qquad U(x,t)=\sum_{m=1}^{\infty}\chi(x)Y_m(t) \tag{21}$$

where m denotes the number of vibration modes and other functions are defined as follows:

$$\eta_m(x),\chi_m(x)=\sin\left(\frac{m\pi x}{l}\right) \qquad f_m(t),Y_m(t)=e^{i\omega t} \tag{22}$$

On the other hand, the other component of response (i.e. rotational angle, ψ), can be written also as:

$$\psi(x,t)=\sum_{m=1}^{\infty}\xi_m(x)g_m(t) \qquad \xi_m(x)=\cos\left(\frac{m\pi x}{l}\right),g_m(t)=e^{i\omega t} \tag{23}$$

Substituting Eqs. (21) and (23) into second and third of Eq. (18), the natural frequency of transverse vibration obtained from the following relation:

$$\omega^4 A_1+\omega^2 B=C \tag{24}$$

where the constants A_1 , B and C are defined as follows:

$$\begin{aligned}
A_1&=\frac{\mu\rho I\pi^2}{L^4}\left(-\mu m_t\pi^2-2m_tL^2\right)-m_t\rho I\\
B&=\frac{mEI\pi^2}{2L^4(1-\nu^2)}\left(\mu\pi^2+L^2\right)+\frac{\mu mk_sGA\pi^2}{L^2}+k_w\rho I\\
&+\frac{\rho I\pi^2}{L^6}\left(L^2\mu^2\pi^2k_w+\mu^2\pi^2G_p+AG\pi^2k_s+2L^4\mu k_w+2L^2\mu\pi^2G_p+L^4G_p+L^4k_sGA\right)\\
C&=\frac{EI\pi^2}{2L^6(1-\nu^2)}\left(L^2\pi^2\mu k_w+\pi^4\mu G_p+L^2\pi^2k_sG+L^4k_w+L^2\pi^2G_p\right)\\
&+\frac{GA\pi^2}{L^4}\left(L^2\mu k_wk_s+L^2\pi^2\mu Gk_s+L^4G_pk_s\right)+GAk_wk_s
\end{aligned} \tag{25}$$

Then the natural frequency of the system during vibrating transversely is:

$$\omega_T=\sqrt{\frac{-B+\sqrt{B^2+4A_1C}}{2A_1}} \tag{26}$$

Using the same procedure for transverse vibration, the following relation specifies natural frequency of longitudinal vibration:

$$\omega_L=\sqrt{\frac{A_2}{S}} \tag{27}$$

where the constant parameters are defined as follows:

$$\begin{aligned}
A_2&=A\left\{\left(\frac{\pi}{l}\right)^2\left(c_{11}+\frac{{h_{11}}^2}{\in_{11}}\right)+\left(\frac{\pi}{l}\right)^4\left(\mu c_{11}+\frac{3\mu {h_{11}}^2}{2\in_{11}}\right)+\left(\frac{\pi}{l}\right)^6\left(\frac{\mu^2{h_{11}}^2}{2\in_{11}}\right)\right\}\\
S&=m_t\left(1+2\left(\frac{\pi}{l}\right)^2\mu+\left(\frac{\pi}{l}\right)^4\mu^2\right)
\end{aligned} \tag{28}$$

In order to obtain maximum deflection of transverse vibration, the following procedure has been traversed:

Substituting Eqs. (21) and (23) into second and third of Eq.(18), multiplying both sides of the resulting equations with $\eta_n(x)$ and $\xi_n(x)$, integrating them over the domain(0,L) yields:

$$\begin{aligned}&\sum_{m=1}^{\infty}\ddot{f}_m\int_0^L\mu\rho A\eta_m''\eta_n dx-\sum_{m=1}^{\infty}f_m\int_0^L\mu G_p\eta_m''\eta_n dx-\mu P''+\sum_{m=1}^{\infty}\ddot{f}_m\int_0^L\mu K_w\eta_m''\eta_n dx+\sum_{m=1}^{\infty}f_m\int_0^L K_s GA\eta_m''\eta_n dx\\&\sum_{m=1}^{\infty}g_m\int_0^L K_s GA\xi_m'\eta_n dx-\sum_{m=1}^{\infty}\ddot{f}_m\int_0^L\rho A\eta_m\eta_n dx-\sum_{m=1}^{\infty}f_m\int_0^L K_w\eta_m\eta_n dx+\sum_{m=1}^{\infty}f_m\int_0^L G_p\eta_m''\eta_n dx+P=0\end{aligned}\tag{29}$$

$$\begin{aligned}&\sum_{m=1}^{\infty}f_m\int_0^L K_s GA\eta_m'\xi_n dx+\sum_{m=1}^{\infty}g_m\int_0^L K_s GA\xi_m\xi_n dx-\sum_{m=1}^{\infty}\ddot{g}_m\int_0^L I\mu\rho\xi_m''\xi_n dx\\&-\sum_{m=1}^{\infty}g_m\int_0^L\frac{EI}{\left(1-\nu^2\right)}\xi_m''\xi_n dx+\sum_{m=1}^{\infty}g_m\int_0^L\rho I\xi_m\xi_n dx=0\end{aligned}\tag{30}$$

Dots and prime over alphabet denote the derivations of the generalized coordinates with respect to t and x, respectively.

According to the following orthogonality condition:

$$\int_0^L\eta_m\eta_n dx=\begin{cases}\dfrac{L}{2} & m=n\\ 0 & m\neq n\end{cases}\tag{31}$$

Based on the Dirac-delta function property:

$$\int_0^L f(x)\delta^n(x-x_{np})\,dx=\begin{cases}(-1)^n f^n(x_0) & x_1<x_0<x_2\\ 0 & otherwise\end{cases}\tag{32}$$

where δ^n shows nth derivative of Dirac-delta function. Rearranging Eqs. (29) and (30) ,the following matrix form of equations are obtained:

$$\begin{bmatrix}M_{11} & 0\\ 0 & M_{22}\end{bmatrix}\begin{Bmatrix}\ddot{f}_m\\ \ddot{g}_m\end{Bmatrix}+\begin{bmatrix}K_{11} & K_{12}\\ K_{21} & K_{22}\end{bmatrix}\begin{Bmatrix}f_m\\ g_m\end{Bmatrix}=\begin{Bmatrix}F_n(t)\\ 0\end{Bmatrix}\tag{33}$$

where $F_n(t)=P_0\left[\mu\chi_n''(x_{np})-\chi_n(x_{np})\right]$ for $0<t<\dfrac{L}{v_{np}}$ and $F_n(t)=0$ for $t>\dfrac{L}{v_{np}}$.

5 NUMERICAL SOLUTION METHODOLOGY

In this paper, a finite element method namely as average acceleration method proposed by Newmark has been used to evaluate time dependent function of normalized dynamic deflection numerically [15]. The following assumptions are used:

$$\dot{U}_{t+\Delta t}=\dot{U}_t+\left[(1-\delta)\ddot{U}_t+\delta\ddot{U}_{t+\Delta t}\right]\Delta t\tag{34}$$

$$U_{t+\Delta t}=U_t+\dot{U}_t\Delta t+\left[\left(\frac{1}{2}-\alpha\right)\ddot{U}_t+\alpha\ddot{U}_{t+\Delta t}\right]\Delta t^2\tag{35}$$

where α and δ are parameters that can be determined to obtain integration stability and accuracy. Newmark originally proposed as an unconditionally stable scheme, the constant average acceleration method (also called trapezoidal rule) in which case $\alpha = \frac{1}{4}$ and $\delta = \frac{1}{2}$.

Indeed, this method is used to obtain displacement, velocity and acceleration fields of a dynamic system under general equilibrium equations which can be shown as matrix form as follows:

$$M\ddot{U}_{t+\Delta t} + C\dot{U}_{t+\Delta t} + KU_{t+\Delta t} = F_{t+\Delta t} \tag{36}$$

where M is mass matrix, K is stiffness matrix and C is damping matrix.

Solving from Eq. (35) for $\ddot{U}_{t+\Delta t}$ in terms of $U_{t+\Delta t}$ and then substituting for $\ddot{U}_{t+\Delta t}$ into Eq. (34), we obtain equations for $\ddot{U}_{t+\Delta t}$ and $\dot{U}_{t+\Delta t}$, each in terms of the unknown displacements $U_{t+\Delta t}$ only. These two relations for $\dot{U}_{t+\Delta t}$ and $\ddot{U}_{t+\Delta t}$ are substituted into Eq. (36) to solve for $U_{t+\Delta t}$, after which, using Eqs. (34) and (35), $\dot{U}_{t+\Delta t}$ and $\ddot{U}_{t+\Delta t}$ can be calculated.

The complete algorithm of this method in order to be used for computer programming is summarized and given in the following table.

A. Initial calculations:

1. Form stiffness matrix K, mass matrix M and C damping matrix.
2. Initialize U_0, $\dot{U}_0$ and $\ddot{U}_0$.
3. Select time step size, parameters α and δ, and calculate integration constants as follows:

$$a_0 = \frac{1}{\alpha\Delta t^2}, a_1 = \frac{\delta}{\alpha\Delta t}, a_2 = \frac{1}{\alpha\Delta t}, a_3 = \frac{1}{2\alpha} - 1, a_4 = \frac{\delta}{\alpha} - 1, a_5 = \frac{\Delta t}{2}\left(\frac{\delta}{\alpha} - 2\right), a_6 = \Delta t\left(1-\delta\right), a_7 = \delta\,\Delta t \tag{37}$$

4. Form effective stiffness matrix $K_e; K_e = K + a_0 M + a_1 C$

B. For each time step:

1. Calculate effective loads at time $t + \Delta t$
2. Solve for displacements at time $t + \Delta t$ using proper direct elimination methods such as Gauss elimination, Gauss-Jordan elimination, the matrix inverse method and Doolittle LU factorization.
3. Calculate the accelerations and velocities at time $t + \Delta t$:

$$\begin{aligned} \ddot{U}_{t+\Delta t} &= a_0\left(U_{t+\Delta t} - U_t\right) - a_2\dot{U}_t - a_3\ddot{U}_t \\ \dot{U}_{t+\Delta t} &= \dot{U}_t + a_6\ddot{U}_t + a_7\ddot{U}_{t+\Delta t} \end{aligned} \tag{38}$$

6 NUMERICAL RESULTS AND DISCUSSION

In this study, the variation of nondimensional fundamental frequencies and normalized dynamic deflection for the various values of nonlocal parameter, elastic and shear medium and velocity parameter is investigated. The properties of the BNNT taken from geometrical, mechanical and electric properties of the system for SWBNNT are considered as [1]: $E = 1.8TPa, \rho = 3487\frac{Kg}{m^3}, R_{in} = 11.43nm, R_{out} = 12.31nm, t = 0.075nm$.

In order to investigate the effect of various parameters discussed in this section, the following dimensionless parameters are defined:

The nondimensional fundamental frequency can be obtained as:

$$\overline{\omega} = \omega \times L^2\sqrt{\frac{\rho A}{EI}} \tag{39}$$

The dimensionless velocity parameter (α) can be expressed as:

$$\alpha = \frac{v_{np}}{v_{cr1}} \tag{40}$$

where $v_{cr1} = \omega_1 L/\pi$ and ω_1 is the first circular frequency. Also, the dimensionless parameter t^* represents dimensionless time and can be defined as:

$$t^* = \frac{x_p}{L} = \frac{v_p t}{L} \tag{41}$$

The normalized dynamic deflection (NDD) may be defined as:

$$NDD = \frac{w(x,t)}{w_{st}},\ w_{st} = \frac{PL^3}{48EI} \tag{42}$$

w_{st} represents the static deflection of nanotube under a point load at the mid-span. As indicated, the parameter e_0 was given as 0.39 which has to be determined from experiments by matching dispersion curves of plane waves [14] and parameter a as the length of a C-C and B-N bond which are 0.142 and 0.145nm, respectively. For CNTs and BNNTs, therefore, the range of $e_0 a = 0 - 2nm$ has been widely used.

In order to validate the present proposed formulations, a comparison between results of the present study with those obtained by Aydogdu [16] is proposed in Table 1. As can be seen, there is no remarkable deviation for all aspect ratio values in a specific nonlocal parameter and acceptable results are achieved between this study and [16].

Table 1
A comparison of nondimensional fundamental frequency between the present study and [16].

L/d	$\mu = (e_0 a)^2$	Present study	[16]
10	0	9.7811	9.7443
	1	9.3210	9.2931
	2	8.9377	8.8994
	3	8.5803	8.5517
	4	8.2704	8.2419
20	0	9.8767	9.8381
	1	9.7532	9.7187
	2	9.6341	9.6036
	3	9.5391	9.4924
	4	9.4280	9.3850
50	0	9.8917	9.8645
	1	9.8714	9.8451
	2	9.8512	9.8258
	3	9.8411	9.8066
	4	9.8112	9.7875

Figs. 2 (a) and (b) indicate nondimensional fundamental transverse and axial frequencies versus aspect ratio for selected values of nonlocal parameters. As it is shown, increase in the values of small scale effect leads to decrease in the magnitudes of transverse and axial frequencies. Also, nondimensional fundamental transverse and axial frequencies increase with the increase in the aspect ratio values

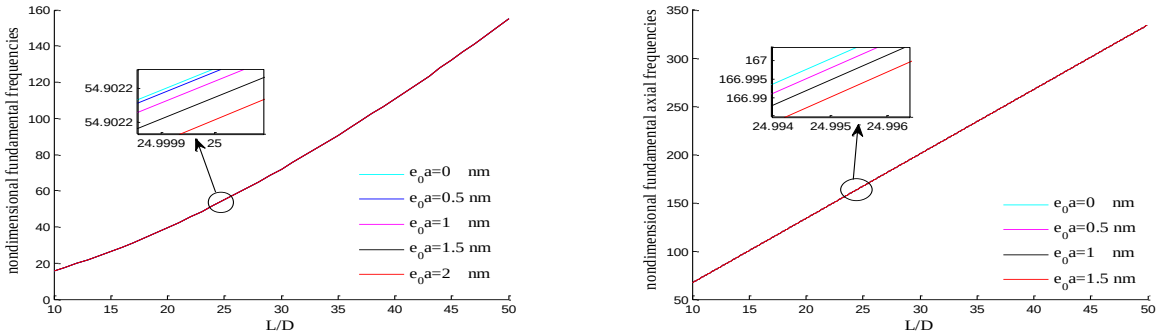

(a) (b)

Fig.2
a)Nondimensional fundamental transverse frequencies versus aspect ratio for various values of nonlocal parameters. b)Nondimensional fundamental axial frequencies versus aspect ratio for various values of nonlocal parameters $\left(G_p = 2.071\ N/m\right)$.

The effect of piezoelasticity on the nondimensional fundamental axial frequencies against aspect ratio is depicted in Fig. 3. It can be concluded that in a specific aspect ratio, the piezoelasticity effect leads to higher axial frequency values.

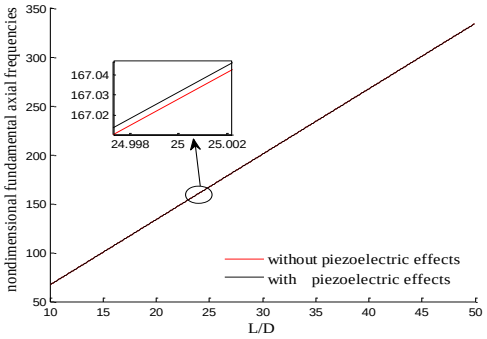

Fig.3
Effect of piezoelectricity on nondimensional fundamental axial frequency $\left(G_p = 2.071\ N/m\right)$.

Fig. 4 demonstrates the influence of surface stress on the nondimensional fundamental transverse frequency versus aspect ratio. The most notable feature in this Figure is the effect of the surface elasticity modulus and the residual surface tension on the transverse frequency. As it is shown, increase in the magnitudes of the surface elasticity modulus and the residual surface tension gives higher values of the transverse frequency.

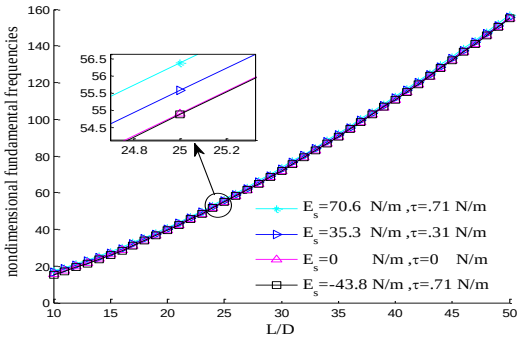

Fig.4
Surface stress effect on the nondimensional fundamental transverse frequencies against aspect ratio.

Fig. 5 gives maximum NDD of SWBNNT and its variation with aspect ratio for various values of small scale effects. For higher values of aspect ratio, NDD converges to a constant value.

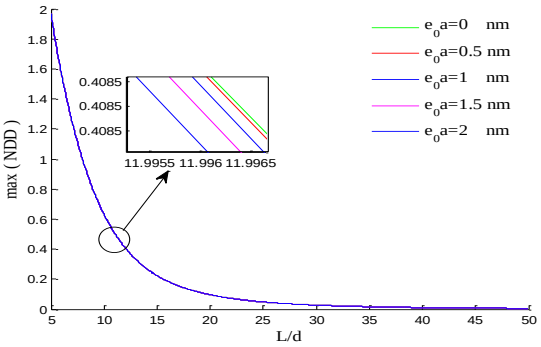

Fig.5
Small scale effect on maximum normalized dynamic deflection ofSWBNNT with aspect ratio.

Fig. 6 shows the variation of maximum normalized dynamic deflection with dimensionless velocity parameter for selected values of the spring modulus and $e_0 a = 1nm$. The most remarkable observation is that with respect to increase in the spring modulus magnitudes, the SWBNNT becomes stiffer. Indeed, the variation of NDD with higher values of spring modulus is found lower than other values.

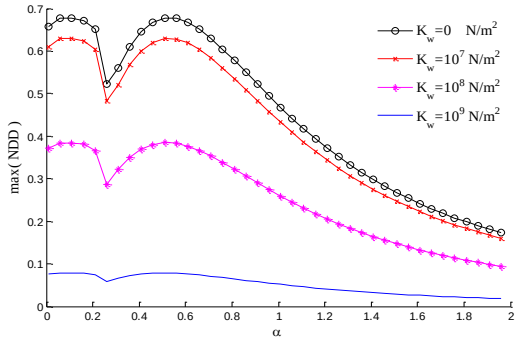

Fig.6
Maximum normalized dynamic deflection of SWBNNT versus velocity parameter for various values of Pasternak constants.

Fig. 7 illustrates the variation of normalized dynamic deflection in comparison with the aspect ratio for various values of shear and spring modulus magnitudes. An interesting observation from this figure is that, the maximum NDD descends considerably with increase in constant parameters of foundation. All of the curves converge to a constant value. This value is lower for the case of SWBNNT with elastic medium. In absence of elastic medium stiffness, maximum NDD has higher values.

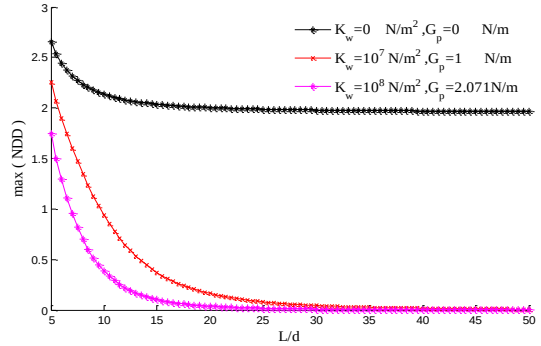

Fig.7
The influence of surrounding elastic medium on the normalized dynamic deflection versus aspect ratio.

The effect of velocity parameter values on the maximum NDD with time history of mid-span is shown in Fig. 8. It is interesting to note that at lower values of the velocity parameter the periodic motion of SWBNNT is more remarkable, whereas with respect to increase in the values of velocity parameter maximum NDD decreases.

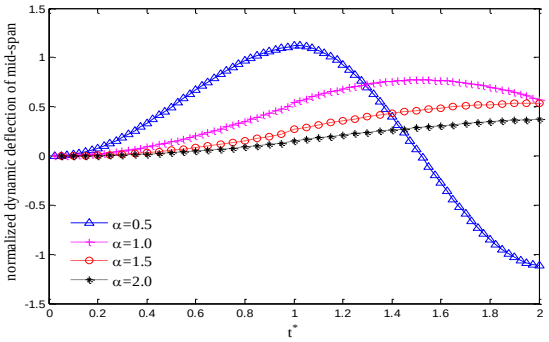

Fig.8
Time histories of mid-span for various values of velocity parameter and $\left(G_p=2.071\ N/m\,,k_w=10^7\ N/m^2\right)$.

The maximum NDD against time history of mid-span vibration for selected shear modulus values for various values of nondimensional velocity parameter is given in Figs. 9 (a), (b), (c) and (d) (i.e. $\alpha=0.5,\alpha=1,\alpha=1.5$ and $\alpha=2$ and $k_w=10^7\ N/m^2$). As illustrated in these figures, the number of oscillations decreases with increase in the value of velocity parameter. Also, the amplitude of normalized dynamic deflection at mid-span decreases with increase in the values of velocity parameter. Indeed, higher values of velocity parameter lead to lower magnitudes of maximum NDD. Also, increase in the values of shear modulus in a specific dimensionless time NDD decreases. Table 2. shows the difference between the values of normalized dynamic deflection of mid-span for various values of velocity parameter and shear modulus.

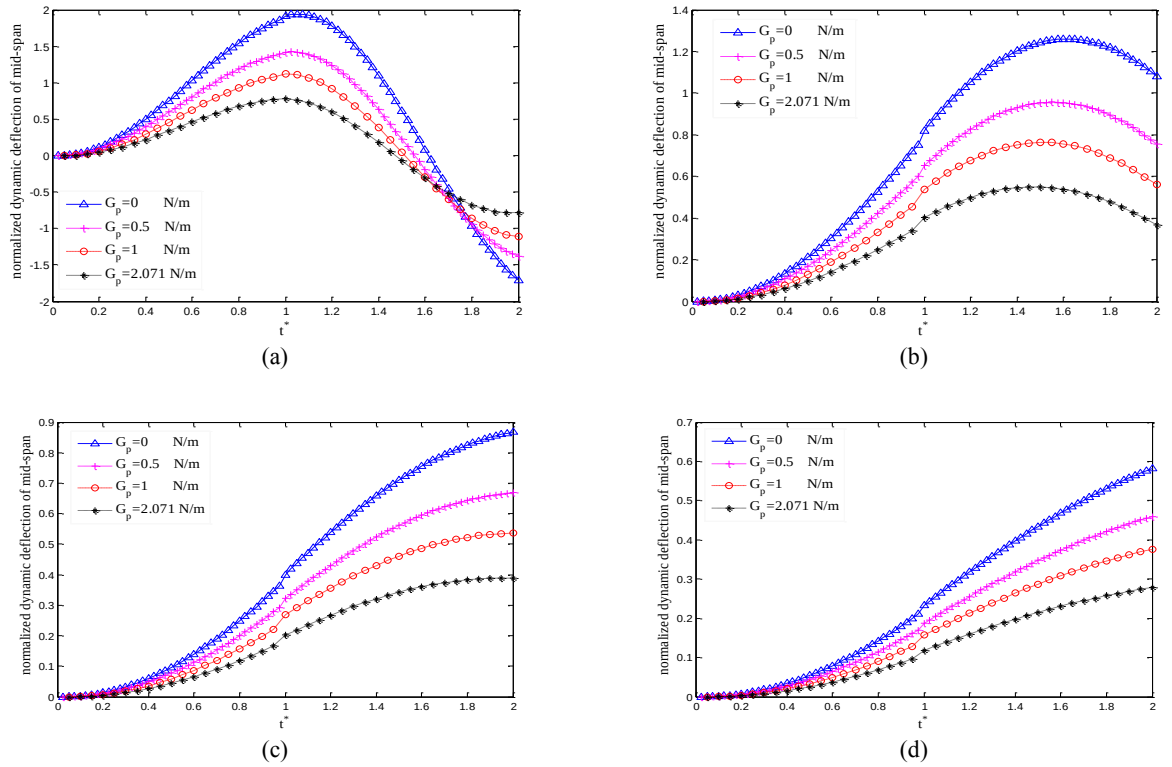

Fig.9
a) Effect of shear modulus on time history of dynamic deflection at mid-span $\alpha=0.5$. b) Effect of shear modulus on time history of dynamic deflection at mid-span $\alpha=1$. c) Effect of shear modulus on time history of dynamic deflection at mid-span $\alpha=1.5$. d) Effect of shear modulus on time history of dynamic deflection at mid-span $\alpha=2$.

Table 2
Variation of normalized dynamic deflection of mid-span with dimensionless time of nanoparticle movement for various values of velocity parameter with Pasternak medium.

α	Dimensionless Time(t^*)	Normalized dynamic deflection of mid-span			
		$Gp = 0$	$Gp = 0.5$	$Gp = 1.5$	$Gp = 2.071$
0.5	0.2	0.1510	0.1220	0.1019	0.0467
	0.4	0.5577	0.4460	0.3707	0.1688
	0.6	1.0958	0.8622	0.7088	0.3188
	0.8	1.6009	1.2284	0.9934	0.4386
	1.0	1.9333	1.4230	1.1052	0.4702
	1.2	1.7233	1.1791	0.8083	0.3196
	1.4	0.9864	0.5339	0.2179	0.0450
	1.6	0.0518	0.2932	0.4515	0.2471
	1.8	1.0743	1.0203	0.9570	0.4433
1.0	0.2	0.0385	0.0312	0.0262	0.0121
	0.4	0.1511	0.1221	0.1023	0.0469
	0.6	0.3289	0.2646	0.2211	0.1011
	0.8	0.5580	0.4463	0.3717	0.1692
	1.0	0.8533	0.6768	0.5788	0.2617
	1.2	1.0764	0.8444	0.7017	0.3144
	1.4	1.2154	0.9385	0.7591	0.3360
	1.6	1.2597	0.9508	0.7460	0.3238
	1.8	1.2057	0.8804	0.6632	0.2796
1.5	0.2	0.0173	0.0140	0.0118	0.0054
	0.4	0.0682	0.0551	0.0463	0.0213
	0.6	0.1511	0.1221	0.1024	0.0469
	0.8	0.2632	0.2120	0.1774	0.0812
	1.0	0.4183	0.3358	0.2916	0.1330
	1.2	0.5546	0.4431	0.3768	0.1712
	1.4	0.6716	0.5333	0.4466	0.2021
	1.6	0.7652	0.6027	0.4975	0.2238
	1.8	0.8322	0.6487	0.5280	0.2353
2.0	0.2	0.0098	0.0079	0.0067	0.0031
	0.4	0.0385	0.0312	0.0262	0.0121
	0.6	0.0860	0.0695	0.0583	0.0268
	0.8	0.1511	0.1221	0.1024	0.0469
	1.0	0.2435	0.1962	0.1712	0.0784
	1.2	0.3281	0.2638	0.2260	0.1033
	1.4	0.4065	0.3257	0.2757	0.1255
	1.6	0.4768	0.3804	0.3186	0.1447
	1.8	0.5378	0.4268	0.3543	0.1603

In Fig. 10, time history of oscillation at mid-span plotted for $\alpha = 0.5$ and $G_p = 2\,N/m$. The effect spring modulus is shown in this figure. As can be seen, increase in values of spring modulus dynamic deflection of mid-span decreases.

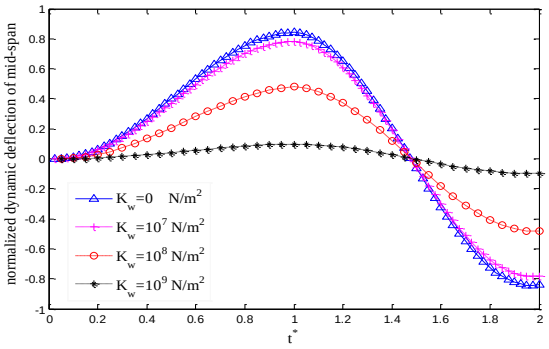

Fig.10
Effect of spring modulus on time history of dynamic deflection at mid-span.

Finally, the variations of both shear and spring modulus of Pasternak medium is shown in Fig.11, simultaneously. It is observed from this figure that the maximum dynamic deflection of mid-span decreases with stiffer Pasternak foundation. Also, with respect to increase in the values of the elastic medium stiffness the maximum NDD decreases. Indeed, the maximum NDD can be found at lower values of dimensionless time.

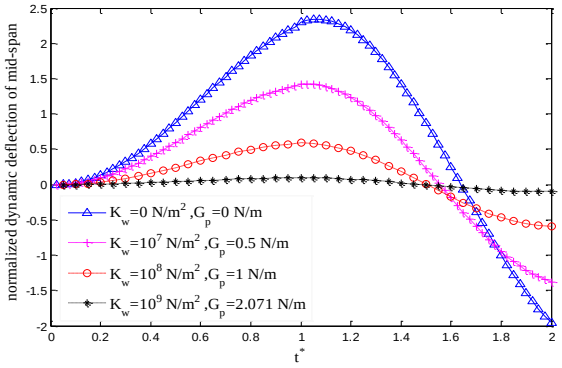

Fig.11
Variation of time history of normalized dynamic deflection at mid-span for various values of spring modulus and shear modulus.

7 CONCLUSIONS

In this study, a semi analytical method was used to achieve formulation of SWBNNT vibration surrounded by a Pasternak foundation under a moving nanoparticle. As it is presented, the comparison of nondimensional fundamental axial and transverse frequencies with respect to aspect ratio and surface stress effects were investigated. Also, the variation of maximum normalized dynamic deflection of SWBNNT and dynamic deflection of mid-span with aspect ratio, dimensionless time of nanoparticle movement and dimensionless velocity parameter for various values of Pasternak medium constants were carried out. The major conclusions obtained are as follows:

- It is demonstrated that the nonlocal parameter effect decreased extremely as diameter and aspect ratio increase. As it is proved, all of the curves are converging to the local state.
- It is observed that an increase in the value of shear modulus leads to a decrease in the maximum normalized dynamic deflection of SWBNNT and normalized dynamic deflection of mid-span. Also, the maximum value of the normalized dynamic deflections for without surrounding Pasternak medium is generally larger than other values of elastic medium stiffness.
- In a specific aspect ratio, the piezoelasticity effect leads to higher axial frequency values.
- The positive and negative deflections show that SWBNNT vibrates under a moving harmonic load.
- At lower values of the velocity parameter the periodic motion of SWBNNT is more remarkable, whereas with respect to increase in the values of velocity parameter maximum NDD decreases.
- The nondimensional fundamental frequencies for the case of with surface stress effects have higher values.
- Increasing the spring modulus magnitudes the SWBNNT becomes stiffer. Indeed, the variation of NDD with higher values of spring modulus is found lower than other values.

- The amplitude of normalized dynamic deflection at mid-span decreases with increase in the values of velocity parameter. Indeed, higher values of velocity parameter lead to lower magnitudes of maximum NDD.
- It can be found from the results that, the effect of shear modulus (G_p) can be considered as a damping element.

ACKNOWLEDGMENTS

The authors are grateful to University of Kashan for supporting this work by Grant No. 363443/34. They would also like to thank the Iranian Nanotechnology Development Committee for their financial.

REFERENCES

[1] Khodami Maraghi Z., Ghorbanpour Arani A., Kolahchi R., Amir S., Bagheri M.R., 2012, Nonlocal vibration and instability of embedded DWBNNT conveying viscose fluid, *Composites: Part B* **45**(1): 423-432.

[2] Simsek M., 2011, Forced vibration of an embedded single-walled carbon nanotube traversed by a moving load using nonlocal Timoshenko beam theory, *Steel and Composite Structures* **11**(1): 59-76.

[3] Simsek M., 2010, Vibration analysis of a single-walled carbon nanotube under action of a moving harmonic load based on nonlocal elasticity theory, *Physica E* **43**(1): 182-191.

[4] Ghorbanpour Arani A., Roudbari M. A., Amir S., 2012, Nonlocal vibration of SWBNNT embedded in bundle of CNTs under moving a nanoparticle, *Physica B* **407**(17): 3646-3653.

[5] Ansari R., Sahmani S., 2011, Bending behavior and buckling of nanobeams including surface stress effects corresponding to different beam theories, *International Journal of Engineering and Science* **49**(11): 1244-1255.

[6] Ansari R., Sahmani S., 2011, Surface stress effects on the free vibration behavior of nanoplates, *International Journal of Engineering and Science* **49**(11): 1204-1215.

[7] Lei X.W., Natsuki T., Shi J.X., Ni Q.Q., 2012, Surface effects on the vibrational frequency of double-walled carbon nanotubes using the nonlocal Timoshenko beam model, *Composites: Part B* **43**(1): 64-69.

[8] Narendar S., Ravinder S., Gopalakrishnan S., 2012, Study of non-local wave properties of nanotubes with surface effects, *Computational Materials Science* **56**:179-184.

[9] Ghorbanpour Arani A., Amir S., Shajari A.R., Mozdianfard M.R., Khoddami Maraghi Z., Mohammadimehr M., 2011, Electro-thermal non-local vibration analysis of embedded DWBNNTs, *Journal of Mechanical Engineering Science* **224**: 745.

[10] Ghorbanpour Arani A., Amir S., Shajari A.R., Mozdianfard M.R., 2012, Electro-thermo-mechanical buckling of DWBNNTs embedded in bundle of CNTs using nonlocal piezoelasticity cylindrical shell theory, *Composites Part B Engineering* **43**: 195-203.

[11] Yang J., 2005, *An Introduction to the Theory of Piezoelectricity*, Springer, Lincoln.

[12] Ghorbanpour Arani A., Kolahchi R., Mosallaie Barzoki A.A., 2011, Effect of material inhomogeneity on electro-thermo-mechanical behaviors of functionally graded piezoelectric rotating cylinder, *Applied Mathematical Modeling* **35**: 2771-2789.

[13] Simsek M., 2010, Dynamic analysis of an embedded microbeam carrying a moving microparticle based on the modified couple stress theory, *International Journal of Engineering Science* **48**: 1721-1732.

[14] Eringen A.C., 1983, On differential equations of nonlocal elasticity and solutions of screw dislocation and surface waves, *Journal of Applied Physics* **54**: 4703.

[15] Bathe K. J., 1982, *Finite Element Procedures in Engineering Analysis*, Prentice-Hall.

[16] Aydogdu M., 2009, A general nonlocal beam theory: Its application to nanobeam bending, buckling and vibration, *Physica E* **41**: 1651-1655.